

Lorenz-like systems and Lorenz-like attractors: Definition, examples, and equivalencesChristophe Letellier^{1,*}, Eduardo M. A. M. Mendes^{2,†} and Jean-Marc Malasoma^{3,‡}¹*Rouen Normandie University—CORIA, Avenue de l'Université, 76800 Saint-Etienne du Rouvray, France*²*Laboratório de Modelagem, Análise e Controle de Sistemas Não Lineares, Universidade Federal de Minas Gerais, Av. Antônio Carlos 6627, 31270-901 Belo Horizonte, MG, Brazil*³*Rue de Frindeau, 69780 Saint Pierre de Chandieu, France*

(Received 29 June 2023; accepted 12 September 2023; published 10 October 2023)

Since the early 1970s, numerous systems exhibiting an algebraic structure resembling that of the 1963 Lorenz system have been proposed. These systems have occasionally yielded the same attractor as the Lorenz system, while in other cases, they have not. Conversely, some systems that are evidently distinct from the Lorenz system, particularly in terms of symmetry, have resulted in attractors that bear a resemblance to the Lorenz attractor. In this paper, we put forward a definition for Lorenz-like systems and Lorenz-like attractors. The former definition is based on the algebraic structure of the governing equations, while the latter relies on topological characterization. Our analysis encompasses over 20 explicitly examined chaotic systems.

DOI: [10.1103/PhysRevE.108.044209](https://doi.org/10.1103/PhysRevE.108.044209)**I. INTRODUCTION**

The Lorenz system [1] is the most-known chaotic system. Its success results from a few specificities which are, among others, (i) it is the first published chaotic system actually recognized for its aperiodic solution which is sensitive to initial conditions, (ii) it is a quite simple set of quadratic equations, (iii) it has strong—although oversimplified—connection with the physical experiment known as the Rayleigh-Bénard experiment [2], and (iv) it produces a very suggestive chaotic attractor which may be viewed as the two wings of a butterfly, thus providing a direct connection with the so-called “butterfly effect.” [3] In fact, Rikitake had previously published a system that exhibits remarkably similar dynamics [4]. However, unlike in Lorenz’s paper, Rikitake did not provide a visual representation of the attractor in a state space projection, and the analysis of the chaotic solution was not as comprehensive. It was only in the early 1970s that a more thorough examination of its chaotic solution was carried out [5]. An experimental realization of the Lorenz dynamics was proposed by Malkus two years later [6] and, then, a slightly different version was derived from laser equations [7]. Many other systems with the same kind of algebraic structure and dynamics were hereafter proposed.

Before proceeding, it is essential to establish a clear distinction between the system—the set of differential equations—and the chaotic attractor itself. On the one hand, the designation “Lorenz-like system” is used when the governing equations being studied share specific characteristics with the Lorenz system, as outlined in detail in Sec. II. On the other hand, for an attractor to be classified as a Lorenz

attractor, it must display topological equivalence to the attractor analyzed in the seminal 1963 Lorenz paper [1], which will be explored in Sec. IV. It is crucial to emphasize that a Lorenz-like attractor can be produced by a system that is not inherently Lorenz-like. Conversely, a Lorenz-like system does not necessarily yield an attractor that is classified as a Lorenz attractor (refer to the definition in Sec. IV).

Multiple distinct approaches exist for defining a generalized Lorenz-like system, as evidenced by various studies [8–11]. Frequently, these approaches result in systems with a considerably larger number of monomials than the original Lorenz system’s seven. In Sec. III, we will delve into the topic and explore how a system with an excessive number of monomials can produce various types of attractors that are not characteristic of a Lorenz attractor. To illustrate this point, we will present two examples of the same system structure capable of producing both Lorenz and Rössler attractors.

II. LORENZ-LIKE SYSTEMS

The Lorenz system was proposed by Lorenz as a strong truncation of a Fourier expansion of the Navier-Stokes equations for describing Rayleigh-Bénard convection [1]. In our analysis, we will only consider this system as a dynamical system, disregarding its physical interpretation. The system consists of quadratic monomials in the right-hand side of the governing equations and exhibits rotational invariance around the z axis. For the sake of simplicity, we adopt the convention that the rotation axis corresponds to the z axis. The chaotic attractor obtained by Lorenz is better known than the corresponding governing equations but, as we will see, most often only its general shape is considered, that is, its two “wings” (sometimes also called “scroll”). Therefore, certain attractors are referred to as Lorenz attractors even though they are not topologically equivalent to the original Lorenz attractor (see, for example, Ref. [12]). Thus, it is important to make

*christophe.letellier@univ-rouen.fr

†emmendes@ufmg.br

‡jmmalasoma@gmail.com

a clear distinction between Lorenz-like systems and Lorenz attractors.

The term ‘‘Lorenz-like attractor’’ will be introduced for designating the attractors often produced by Lorenz-like systems. The present section is devoted to define Lorenz-like system and Sec. IV will discuss what should be meant by Lorenz attractor and, more generally, by Lorenz-like attractor. We will see that the number of singular points is not a key property for producing a two-wing attractor. This is not therefore retained in our definition.

We will begin by presenting a definition of what is meant by a Lorenz-like system in this context.

Definition 1. A Lorenz-like system is a quadratic three-dimensional system with an order-2 rotation symmetry and whose part of the rotation axis has a transverse stability of the saddle type.

While the origins of the first two properties are obvious, the third property, namely, the transverse stability of the saddle type, is required for getting the tearing mechanism involved in the production of an attractor bounded by a genus-3 torus (see below) [13,14].

Remark 1. In Sec. III, it will be shown that a system with more than seven monomials in the right-hand side of the governing equations can produce a Lorenz attractor as well as a Rössler attractor. The presence of too many monomials allows the equations to produce a wide range of dynamics and we argue that it becomes meaningless to speak of a Lorenz-like system. We will therefore add a restriction to our definition: only system with less than eight monomials are considered.

Remark 2. As a convention, the z axis is designated as the rotation axis. When a linear governing equation is present (such as in the first equation of the Lorenz system), it is consistently associated with the x variable. This association is chosen because it provides the simplest jerk function when it exists (this is always the case in the examples here considered), which corresponds to the best observability of the state space [15]. Therefore, comparing the jerk function F_x is sufficient to determine the jerk-equivalence between Lorenz-like systems [16]. Let us designate this form as the standard form.

Remark 3. It is known that at least five monomials are required for producing chaos. The Lorenz system itself has seven monomials and it cannot be considered as not being a Lorenz-like system! When a system has more than seven monomials, it can produce a huge variety of chaotic attractors which are very often much more complex than the Lorenz or the Burke and Shaw systems. To us, these systems thus lose their specificities and there is no longer any interest in considering them as having some specific properties of the Lorenz system.

Consequently, a Lorenz-like system has the form

$$\begin{aligned} \dot{x} &= \alpha_{11}x + \alpha_{12}y + \alpha_{16}xz + \alpha_{18}yz, \\ \dot{y} &= \alpha_{21}x + \alpha_{22}y + \alpha_{26}xz + \alpha_{28}yz, \\ \dot{z} &= \alpha_{30} + \alpha_{33}z + \alpha_{34}x^2 + \alpha_{35}xy + \alpha_{37}y^2 + \alpha_{39}z^2, \end{aligned} \tag{1}$$

where the first two equations are made of odd monomials and the third equation with at least one even monomial of the form $x^i y^j$ with $i + j$ even. This is the general form already retained by one of us [17]. Given our limitation to systems

with fewer than eight monomials, it implies that no more than seven of the α_{ij} coefficients are zero. The resulting form automatically ensures that a Lorenz-like system is equivariant under a rotation symmetry $\mathcal{R}_z(\pi)$, that is, it obeys to [18]

$$\Gamma \cdot f(\mathbf{x}) = f(\Gamma \cdot \mathbf{x}), \tag{2}$$

where

$$\Gamma = \begin{bmatrix} -1 & 0 & 0 \\ 0 & -1 & 0 \\ 0 & 0 & +1 \end{bmatrix}. \tag{3}$$

Note that we cannot introduce the constant monomial α_{20} in the second equation, as was done in Refs. [19] and [20], since it would break the rotation symmetry. The second part of the definition can be checked by using the set of 1-regular points as introduced by two of us [21] for determining the range of the rotation axis which has a transverse stability of the saddle type, that is, the required condition for having a tearing mechanism in the neighborhood of the rotation axis [22]. Typically, a tearing is induced by a saddle point and is responsible for a nondifferentiable critical point as the cusp point of the Lorenz map. Therefore, to proceed, we will begin by verifying whether the Lorenz system can be classified as a Lorenz-like system.

The Lorenz system is associated with three governing equations composed of seven monomials, with its algebraic structure described below [1]:

$$\begin{aligned} \dot{x} &= \alpha_{11}x + \alpha_{12}y, \\ \dot{y} &= \alpha_{21}x + \alpha_{22}y + \alpha_{26}xz, \\ \dot{z} &= \alpha_{33}z + \alpha_{35}xy. \end{aligned} \tag{4}$$

The system has actually the properties required for a Lorenz-like system since: (i) it is equivariant [condition (2)] under the matrix Γ which defines a rotation symmetry $\mathcal{R}_z(\pi)$ around the z axis, and (ii) the set of 1-regular points defined by $\dot{x} = \dot{y} = 0$ is the z axis whose transverse stability is of a saddle type for some z values. This is determined from the Jacobian matrix [21]

$$J_{xy} = \begin{bmatrix} -\sigma & +\sigma \\ R - z & -1 \end{bmatrix}. \tag{5}$$

The corresponding eigenvalues

$$\lambda_{\pm} = \frac{-(\sigma + 1) \pm \sqrt{(\sigma - 1)^2 + 4\sigma(R - z)}}{2} \tag{6}$$

are real when

$$z \leq R + \frac{(\sigma - 1)^2}{4\sigma} = 30.025 \tag{7}$$

and

$$\lambda_+ \lambda_- = \sigma(z - R + 1) \tag{8}$$

implies that they are of opposite signs if and only if

$$z < R - 1. \tag{9}$$

Since Eq. (9) implies Eq. (7), the Lorenz system (4) is indeed a Lorenz-like system. Considering the typical parameter values

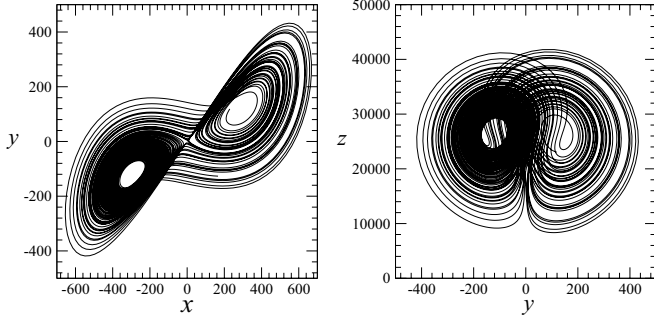


FIG. 1. The chaotic attractor generated by modifying some of the parameter values in the original Lorenz system (4): $\alpha_{11} = 10$, $\alpha_{12} = 25$, $\alpha_{21} = 28$, $\alpha_{22} = 3.5$, $\alpha_{26} = 0.001$, $\alpha_{33} = \frac{8}{3}$, and $\alpha_{35} = 2.0$

[1],

$$\begin{aligned} \alpha_{11} &= -\sigma_L = -10, & \alpha_{12} &= \sigma_L = 10, \\ \alpha_{21} &= R_L = 28, & \alpha_{22} &= -1, & \alpha_{26} &= -1, \\ \alpha_{33} &= -b_L = -\frac{8}{3}, & \alpha_{35} &= +1, \end{aligned} \quad (10)$$

the rotation axis has a transverse stability of a saddle type when $z < 27$.

There are no specific constraints on the parameter values, allowing for the possibility of random modifications. For instance, although the values of α_{22} , α_{26} , and α_{35} , are commonly set to the unity in the Lorenz system (4), we changed them to $\alpha_{22} = 3.5$, $\alpha_{26} = 0.001$, and $\alpha_{35} = 2.0$, and broke the equality between α_{11} and α_{12} by changing the second parameter to $\alpha_{12} = 25$: the chaotic attractor still has the typical shape of the Lorenz attractor (Fig. 1). In this example, the coefficient α_{26} is quite small, but it is not possible to set it to zero. In fact, if α_{26} is set to 0, then the subsystem in x and y is linear and z can be written as a function of time t in the third equation: chaos is therefore not possible in this case. Indeed, the monomial $\alpha_{26}xz$ is present in all the Lorenz-like systems investigated here. This example demonstrates the robustness of the Lorenz attractor in the Lorenz system—which will be defined in the subsequent sections of this paper—against certain variations in the parameter values.

III. RELEVANCE OF PARSIMONIOUS SYSTEMS

When the differential embedding is constructed from the variable x , the Lorenz system can be expressed in a canonical (or jerk) form

$$\begin{aligned} \dot{X} &= Y, \\ \dot{Y} &= Z, \\ \dot{Z} &= F_x, \end{aligned} \quad (11)$$

with

$$\begin{aligned} F_x &= (\alpha_{11}\alpha_{22} - \alpha_{12}\alpha_{21})\alpha_{33}X - (\alpha_{11} + \alpha_{22})\alpha_{33}Y \\ &+ (\alpha_{11} + \alpha_{22} + \alpha_{33})Z - \alpha_{11}\alpha_{26}\alpha_{35}X^3 + \alpha_{26}\alpha_{35}X^2Y \\ &- (\alpha_{11} + \alpha_{22})\frac{Y^2}{X} + \frac{YZ}{X}, \end{aligned} \quad (12)$$

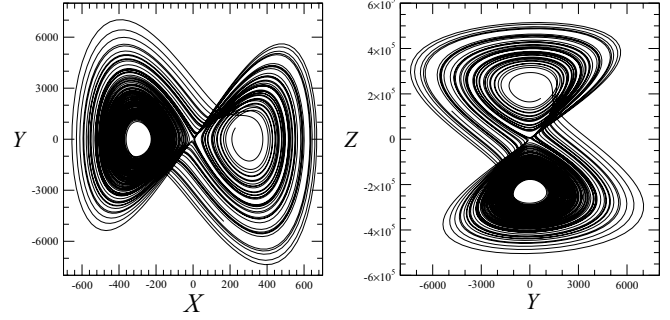


FIG. 2. The chaotic attractor produced by the Lorenz system rewritten in the jerk form (4). Same parameter values as in Fig. 1.

where $X = x$, $Y = \dot{x}$, and $Z = \ddot{x}$. In this case, the rotation symmetry $\mathcal{R}_z(\pi)$ is transformed into an inversion symmetry with respect to the origin of the state space (Fig. 2) [13,18]. According to the definition 1, the jerk form induced by the variable x of the Lorenz system (4) is not a Lorenz-like system because it has (i) an inversion symmetry, (ii) two cubic monomials, and (iii) two rational monomials.

Since the coordinate transformation

$$\Phi_x = \begin{cases} X \mapsto x, \\ Y \mapsto \alpha_{11}x + \alpha_{12}y, \\ Z \mapsto (\alpha_{11}^2 + \alpha_{12}\alpha_{21})x + (\alpha_{11}\alpha_{12} - \alpha_{12}\alpha_{21})y \\ \quad - \alpha_{12}\alpha_{26}xz. \end{cases} \quad (13)$$

has a Jacobian matrix whose determinant vanishes in $X = 0$, Φ_x defines a local diffeomorphism. In that case, the singular observability manifold correspond to a single plane $x = 0$ which allows to change the nature of the symmetry.

Let us now consider the coordinate transformation

$$\Phi = \begin{cases} x \mapsto x, \\ y \mapsto \xi_3 y + \xi_4 z, \\ z \mapsto \xi_5 + \xi_7 y + \xi_8 z \end{cases} \quad (14)$$

whose Jacobian matrix is

$$J_\Phi = \begin{bmatrix} 1 & 0 & 0 \\ 0 & \xi_3 & \xi_4 \\ 0 & \xi_7 & \xi_8 \end{bmatrix}. \quad (15)$$

The determinant is given by

$$\text{Det } J_\Phi = \xi_3 \xi_8 - \xi_7 \xi_4$$

and is only null for a set of coefficients with null measure. In general, Φ defines a diffeomorphism that possesses the property of leaving the variable x unaltered.

When this coordinate transformation is applied to the Lorenz system (4), the following model is obtained

$$\begin{aligned} \dot{x} &= -\sigma x + \sigma \xi_3 y + \sigma \xi_4 z, \\ \dot{y} &= [+b\xi_4\xi_5 + \xi_8(R - \xi_5)]x + (b\xi_4\xi_7 - \xi_3\xi_8)y \\ &+ \xi_4\xi_8(b - 1)z - (\xi_3\xi_4 + \xi_7\xi_8)xy \\ &- (\xi_4^2 + \xi_8^2)xz]/(\xi_3\xi_8 - \xi_4\xi_7), \end{aligned}$$

$$\begin{aligned} \dot{z} = & [-b\xi_3\xi_5 + \xi_7(\xi_5 - R)x + \xi_3\xi_7(1 - b)y \\ & + (\xi_4\xi_7 - b\xi_3\xi_8)z + (\xi_3^2 + \xi_7^2)xy \\ & + (\xi_3\xi_4 + \xi_7\xi_8)xz]/(\xi_3\xi_8 - \xi_4\xi_7), \end{aligned} \quad (16)$$

which is therefore diffeomorphically equivalent to the original Lorenz system when $\xi_3\xi_8 \neq \xi_7\xi_4$. This system has the algebraic structure

$$\begin{aligned} \dot{x} &= \beta_{11}x + \beta_{1,2}y + \beta_{13}z, \\ \dot{y} &= +\beta_{20} + \beta_{21}x + \beta_{22}y + \beta_{23}z \\ &+ \beta_{25}xy + \beta_{26}xz, \\ \dot{z} &= \beta_{30} + \beta_{31}x + \beta_{32}y + \beta_{33}z \\ &+ \beta_{35}xy + \beta_{36}xz, \end{aligned} \quad (17)$$

with 15 monomials, among which four are nonlinear. The rotation symmetry is broken (for instance by the monomial $\beta_{13}z$). It is important to note that there are constraining relationships between the parameters β_i : some of them are not independent of the others as seen in Eq. (16). Strictly speaking, this system does not align with our definition of a Lorenz-like system due to the excessive number of monomials with interdependent coefficients.

Setting the values of ξ_i to arbitrary values, the resulting transformation, expressed as follows:

$$\Phi = \begin{cases} x' \mapsto x, \\ y' \mapsto -\frac{59}{10}y + \frac{83}{10}z, \\ z' \mapsto \frac{23}{10} + \frac{83}{10}y - \frac{177}{10}z, \end{cases} \quad (18)$$

can be applied to the original Lorenz system (4) with the common parameter values (10) to get

$$\begin{aligned} \dot{x}' &= -10x' - 59y' + 83z', \\ \dot{y}' &= +\frac{7636}{5331} - \frac{45489}{3554}x' + \frac{23783}{10662}y' - \frac{24485}{3554}z' \\ &+ \frac{9794}{1777}x'y' - \frac{19109}{1777}x'z', \\ \dot{z}' &= \frac{5428}{5331} - \frac{21331}{3554}x' + \frac{24485}{10662}y' - \frac{20959}{3554}z' \\ &+ \frac{5185}{1777}x'y' - \frac{9794}{1777}x'z'. \end{aligned} \quad (19)$$

The coordinate transformation Φ defines a global diffeomorphism since $\text{Det } J_\Phi = -\frac{59}{10} \times \frac{177}{10} - \frac{87}{10} \times \frac{84}{10} \neq 0, \forall \mathbf{x} \in \mathbb{R}^3$. Since variable x of this transformed Lorenz system is left unchanged by the coordinate transformation Φ , the jerk form of system (19) is necessarily the same as the jerk function (12) obtained for the Lorenz system and its parameter values are also the same. Therefore, these two systems are jerk-equivalent and, consequently, diffeomorphically equivalent.

According to definition 1, the system (19) is not a Lorenz-like system due to the monomial $\frac{9794}{1777}xy$ in the equation f_y and the monomial $-\frac{9794}{1777}xz$ in the equation f_z , since both break the rotation symmetry. Although the rotation symmetry is no longer present, there is still a relationship between the two wings, as exhibited by the differential embedding induced by variable x . A plot of the attractor in one of the plane projection of the state space $\mathbb{R}^3(x', y', z')$ reveals the two wings but not the symmetry that they may have (Fig. 3, left). Nevertheless,

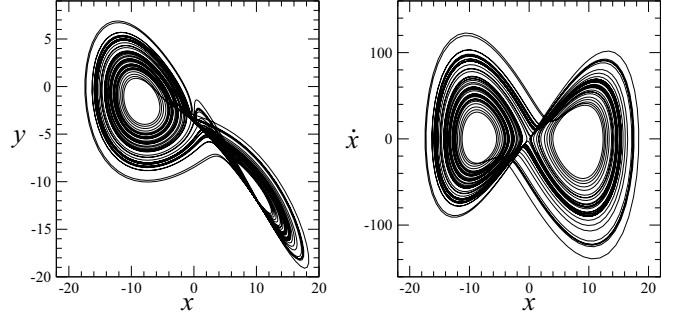


FIG. 3. The transformed Lorenz system (19) with the coordinate transformation Φ (18). The attractor is diffeomorphically equivalent to the original Lorenz attractor but its rotation symmetry is broken. Nevertheless, the relationship between the two wings can still be exhibited in the x -differential embedding (right).

since variable $x' = x$ an order-2 symmetry may still be exhibited (Fig. 3, right). This representation of the attractor is in fact exactly the same as the one induced by the variable x of the Lorenz system. Consequently, a system which is not Lorenz-like can produce a Lorenz attractor.

Now, let us shift our focus to the Rössler system [23]

$$\begin{aligned} \dot{x} &= \alpha_{12}y + \alpha_{13}z, \\ \dot{y} &= \alpha_{21}x + \alpha_{22}y, \\ \dot{z} &= \alpha_{30} + \alpha_{33}z + \alpha_{36}xz, \end{aligned} \quad (20)$$

with $\alpha_{22} = -1, \alpha_{23} = -1, \alpha_{21} = 1, \alpha_{22} = a, \alpha_{30} = b, \alpha_{33} = -c, \alpha_{35} = -1$ to produce the common Rössler attractor (Fig. 4). This system is obviously not a Lorenz-like system. When the coordinate transformation

$$\Phi_x = \begin{cases} X \mapsto x, \\ Y \mapsto \alpha_{12}y + \alpha_{13}z, \\ Z \mapsto \alpha_{13}\alpha_{30} + \alpha_{12}\alpha_{21}x + \alpha_{12}\alpha_{22}y \\ \quad + \alpha_{13}\alpha_{33}z + \alpha_{13}\alpha_{36}xz \end{cases} \quad (21)$$

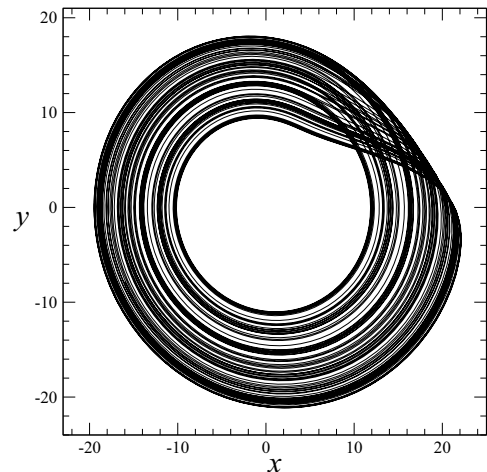


FIG. 4. Rössler attractor produced by the Rössler system (20). Parameter values: $\alpha_{22} = -1, \alpha_{23} = -1, \alpha_{21} = 1, \alpha_{22} = a = 0.1, \alpha_{30} = b = 0.1, \alpha_{33} = -c = -14, \text{ and } \alpha_{35} = -1$.

is applied to the Rössler system, it can be rewritten in the canonical form (11) with

$$F_x = [K_0 + K_1 X + K_2 Y + K_3 Z + K_4 X^2 + K_5 XY + K_6 XZ + K_7 Y^2 + K_8 YZ + K_{10} X^3 + K_{11} X^2 Y + K_{12} X^2 Z] / (\beta_1 + \beta_2 X), \quad (22)$$

which has obviously a different structure from the jerk function (12) obtained for the Lorenz system.

Let us now apply the coordinate transformation

$$\Phi = \begin{cases} x \mapsto x, \\ y \mapsto \xi_2 x + \xi_3 y + \xi_4 z, \\ z \mapsto \xi_7 y + \xi_8 z \end{cases} \quad (23)$$

to the Rössler system (20). The Jacobian matrix is

$$J_\Phi = \begin{bmatrix} 1 & 0 & 0 \\ \xi_2 & \xi_3 & \xi_4 \\ 0 & \xi_7 & \xi_8 \end{bmatrix}, \quad (24)$$

and the determinant is equal to

$$\text{Det } J_\Phi = \xi_3 \xi_8 - \xi_7 \xi_4,$$

that is, it is only null for a set of coefficients with null measure. In general, Φ defines a diffeomorphism that presents the characteristic of leaving the variable x unchanged. The Rössler system thus becomes

$$\begin{aligned} \dot{x} &= -\xi_2 x - (\xi_3 + \xi_7) y - (\xi_4 + \xi_8) z, \\ \dot{y} &= -b\xi_4 + \xi_8(1 + (a + \xi_2)\xi_2)x \\ &\quad + (\xi_8(a\xi_3 + (\xi_3 + \xi_7)\xi_2) + c\xi_4\xi_7)y \\ &\quad + \xi_8(\xi_4(a + c + \xi_2) + \xi_2\xi_8)z \\ &\quad - \xi_4\xi_7 xy - \xi_4\xi_8 xz / (\xi_3\xi_8 - \xi_4\xi_7), \\ \dot{z} &= +b\xi_3 - \xi_7(1 + (a + \xi_2)\xi_2)x \\ &\quad - \xi_7(\xi_3(a + c + \xi_2) + \xi_2\xi_7)y \\ &\quad - (\xi_7(\xi_2(1 + \xi_8) + a\xi_4) + c\xi_3\xi_8)z \\ &\quad + \xi_3\xi_7 xy + \xi_3\xi_8 xz / (\xi_3\xi_8 - \xi_4\xi_7), \end{aligned} \quad (25)$$

that is, a system which has the same algebraic structure as system (16) but with different interplay between the parameter values. To state about a possible equivalence between two systems, it is therefore relevant to investigate how their parameter values are inter-related.

Let us now apply the particular coordinate transformation

$$\Phi = \begin{cases} x \mapsto x, \\ y \mapsto \frac{1}{5}x + \frac{42}{5}y - \frac{19}{5}z, \\ z \mapsto -\frac{3}{10}y + \frac{98}{5}z \end{cases} \quad (26)$$

to the Rössler system (20). We thus obtain the system

$$\begin{aligned} \dot{x} &= -\frac{1}{5}x + \frac{87}{10}y - \frac{79}{5}z, \\ \dot{y} &= -\frac{19}{8289} - \frac{5194}{41445}x + \frac{2884}{13815}y + \frac{247058}{41445}z \\ &\quad + \frac{19}{2763}xy - \frac{3724}{8289}xz, \\ \dot{z} &= +\frac{14}{2763} - \frac{53}{27630}x + \frac{2003}{9210}y - \frac{384299}{27630}z \\ &\quad - \frac{14}{921}xy + \frac{2744}{2763}xz, \end{aligned} \quad (27)$$

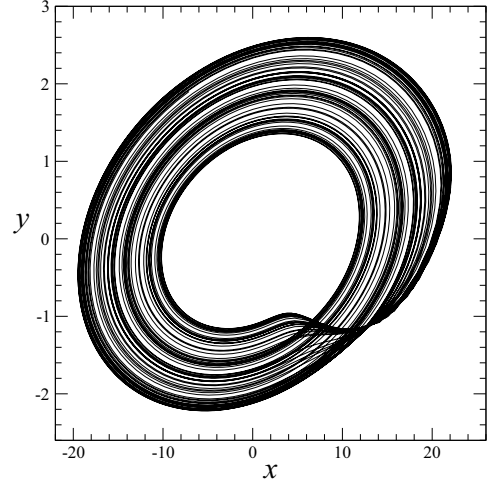


FIG. 5. The rewritten Rössler system (20) with the coordinate transformation Φ (26). The attractor is diffeomorphically equivalent to the original Rössler attractor.

which has the same algebraic structure as the system (19) but which produces a Rössler attractor (Fig. 5) rather than a Lorenz attractor. Since the Lorenz attractor is not diffeomorphically equivalent to the Rössler attractor, this result shows that, when the number of monomials in the governing equations is sufficiently large, it is possible to produce any kind of attractor with a given algebraic structure: what counts is the relationships between the parameter values. The consequences of this are as follows. First, as the number of monomials in the governing equations increases, the algebraic structure becomes less meaningful. Second, since systems (19) and (27) have the same algebraic structure, both have the same jerk form but with different coefficient values: they are therefore not jerk-equivalent and, consequently, not diffeomorphically equivalent. It is important to emphasize that the class of equivalence determined by the structure of the jerk function, in this case, the function (12), encompasses a larger set of systems than the class of diffeomorphic equivalence. Since the Lorenz and the Rössler systems lead to different constraints on the coefficients, their governing equations cannot be diffeomorphically equivalent [16]. With the two examples treated in this section, we showed that the equivalence of the algebraic structure of jerk functions defines a too wide class of dynamical systems. The structure of the system (17) [or equivalently of the system (27)] has 15 monomials: this structure is already too “flexible,” as it encompasses various types of dynamics that can be produced. This is why only parsimonious systems, characterized by no more than seven monomials in their governing equations, are considered here.

IV. TOPOLOGY OF LORENZ-LIKE ATTRACTORS

According to the recently developed dynamical taxonomy by Letellier and co-workers [24], a dynamical taxon achieves complete characterization when a three-dimensional attractor produced by a dissipative is provided with the template. Consequently, in this study, the templates for the typical chaotic

attractors encountered in Lorenz-like systems will be presented. Since the rotation symmetry is considered as a relevant property for Lorenz-like systems, it must also be present in the Lorenz-like attractors.

A. The Lorenz attractor

For the Lorenz attractor initially investigated by Lorenz in 1963, an important ingredient is the ‘‘Lorenz map’’ [Fig. 10(a)], that is, a unimodal map with a cusp at the critical point [1]. This is the first-return map that Lorenz computed from the successive maxima of the z variable. Strictly speaking, this Lorenz map is the first-return map to the two-component Poincaré section [18],

$$\mathcal{P}_{z_{\max}} \equiv \left\{ (y_n, z_n) \in \mathbb{R}^n \mid x_+ = +\sqrt{b(R-1)}, \dot{x}_n < 0 \right\} \cup \left\{ (y_n, z_n) \in \mathbb{R}^n \mid x_- = -\sqrt{b(R-1)}, \dot{x}_n > 0 \right\} \quad (28)$$

There is one component in each wing of the Lorenz attractor. These two components are merged into a single one because the z variable is invariant under the rotation symmetry: As a consequence, it is not possible to determine, from this map, in which wing is the trajectory. This is unveiled by plotting y_{n+1} as a function of y_n rather than z_{n+1} as a function of z_n : For an optimized representation, the two intervals are normalized within unit interval each, one wing within $] -1, 0[$ and the other within $] 0, +1[$ [Fig. 6(c)].

The need for a two component Poincaré section can be derived from a general approach characterizing attractors with bounding tori [14,25]. Indeed, the Lorenz attractor [Fig. 6(a)] is bounded by a genus-3 torus [Fig. 6(b)] as follows. The central hole of this torus is associated with the rotation axis which has a transverse stability of the saddle type in the neighborhood of the attractor, the two other holes are each shaped by the unstable manifold of one of the two symmetry-related singular points which is of the focus type. According to the structure of bounding tori [14], the former hole is of the saddle type and is drawn as a square, and the latter are of the focus type and are drawn as circle. It can be shown that the Poincaré section of an attractor, bounded by a genus- g torus, has $(g - 1)$ components, when $g > 2$, drawn between the peripheral boundary and the boundary of one of the holes of a focus type [14]. Running along the peripheral boundary, there is one component each time there is a hole of the focus type (after one hole of the saddle type, when $g > 2$). It may happen that there are more than one component between a hole of the focus type and the peripheral boundary (see examples in Ref. [14]). Thus, a genus-3 torus requires a two-component Poincaré section defined, for instance, as $\mathcal{P}_{z_{\max}}$ with the y variable or as

$$\mathcal{P}_{\pm} \equiv \{(x_n, y_n) \in \mathbb{R}^2 \mid z_n = R - 1, \dot{z}_n > 0, x_n \gtrless 0\}. \quad (29)$$

The first-return map is conveniently computed with a normalized variable ρ_n obtained from variable x_n (y_n) projected in the unit interval $] -1; 0[$ for \mathcal{P}_- and the unit interval $] 0; +1[$ for \mathcal{P}_+ , the left boundary of each interval being associated with the interior of each wing [22,26]. According to this map [Fig. 6(c)], the branches are ordered as

$$\bar{0} \triangleleft \bar{1} \triangleleft 0 \triangleleft 1,$$

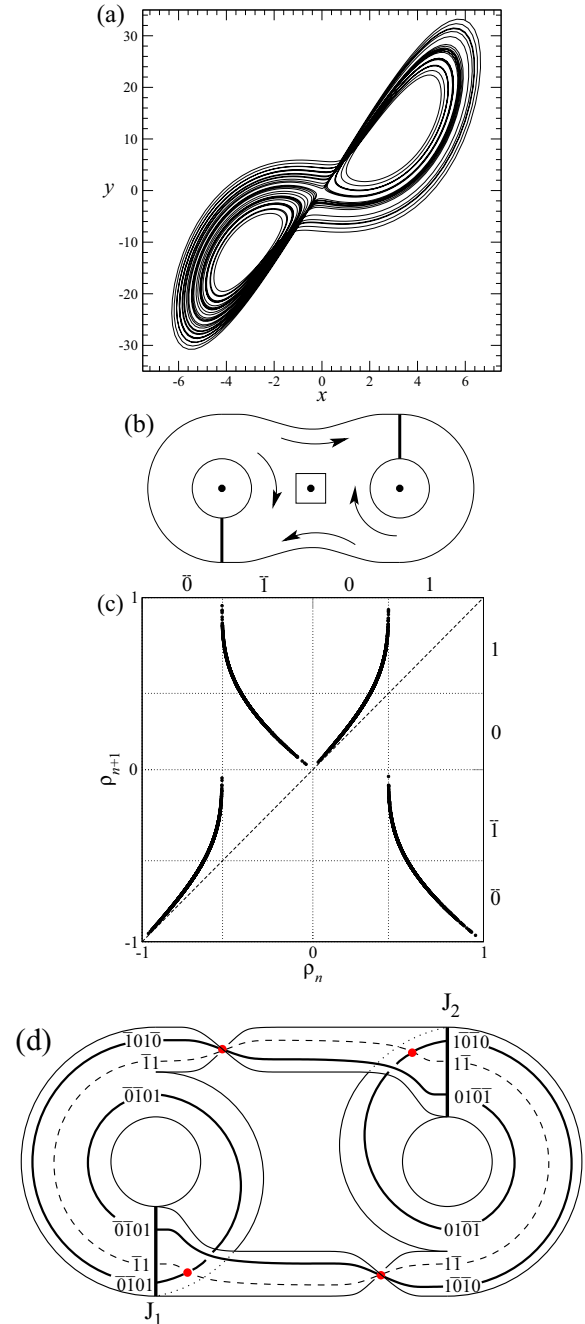


FIG. 6. (b) Genus-3 torus bounding the Lorenz attractor (a): (c) the first-return map to the two-component Poincaré section built from the normalized variable ρ_n (see the main text), and (d) the template describing the topology of the Lorenz attractor produced by the Lorenz system (4). The periodic orbits $(1\bar{0}\bar{1})$ and $(1\bar{0}\bar{1})$ are drawn in the template. Parameter values: $R_L = 28$, $\sigma_L = 10$, and $b_L = \frac{8}{3}$.

where $\bar{0} \triangleleft \bar{1}$ means branch $\bar{0}$ is at the left of branch $\bar{1}$. Branch $\bar{0}$ ($\bar{1}$) is mapped into 0 (1) under the rotation symmetry.

A chaotic attractor can be viewed as a branched manifold is exhibited by Lorenz when he drew the surface associated with the isopleths (see Fig. 3 in Ref. [1]). Branched manifolds were then formally introduced by Williams and then developed by Rössler [27], Birman and Williams [28], Mindlin and

Gilmore [29–31], and Tuffillaro [32]. Chaotic attractors were thus sketched as template made of splitting chart, strips which are twisted and permuted, and joining charts. We showed that the Lorenz attractor has two joining lines (one per component of the Poincaré section) [26,33]. Between two joining lines, there are one splitting chart, strips, and one joining chart. In the template, there is one strip per branch of the first-return map. If we adopt the convention that from the joining line J_1 are issued the strips $\bar{0}$ and $\bar{1}$ and from the joining line J_2 there are strips 0 and 1, thus strips $\bar{0}$ and 1 (0 and $\bar{1}$) are joined at the joining line J_1 (J_2). The template for the Lorenz attractor is drawn in Fig. 6(d) [13] and can be described by the following linker:

$$\mathcal{L}_L = \begin{bmatrix} 0 & 0 & 0 & 0 \\ 0 & +1 & 0 & 0 \\ 0 & 0 & 0 & 0 \\ 0 & 0 & 0 & +1 \end{bmatrix}, \quad (30)$$

where on-diagonal element L_{ii} is the local torsion of the i th strip, and L_{ij} is the permutations between the i th and the j th strips [32,34].

For a genus-1 attractor, this $N_s \times N_s$ matrix is sufficient to encode the way the strips are merged at the joining lines when the standard insertion convention is adopted [32,35]: strips are squeezed from the left to the right, and from the bottom to the top [33]. This is a $N_s \times N_s$ matrix where N_s is the number of strips, equal to the number of branches of the first-return map. When the attractor is characterized by a multicomponent Poincaré section, the linker must have a companion, a *joining* matrix describing how the different strips are merged at each joining chart J_i . This is a $N_j \times N_s$ matrix where N_j is the number of joining charts. By considering the template depicted in Fig. 6(d), the following is obtained:

$$J_{ij} = \begin{bmatrix} 1 & \cdot & \cdot & 2 \\ \cdot & 2 & 1 & \cdot \end{bmatrix}, \quad (31)$$

where i is the label of the i th joining chart and j the label of the j th branch. Thus, $J_{1\bar{0}} = 1$ and $J_{11} = 2$ mean that the strips $\bar{0}$ (bottom) and 1 (top) are squeezed at the first joining chart J_1 . Similarly, strip 0 (bottom) and $\bar{1}$ (top) are squeezed at J_2 . The template of Fig. 6(d) determine completely the topology of the Lorenz attractor.

B. The Burke and Shaw attractor

As explained in Sec. II, there is another attractor which is topologically inequivalent to the Lorenz attractor and often observed in Lorenz-like systems. This is the Burke and Shaw attractor [36] which was discovered in the system proposed by Bill Burke and Robert Shaw [37] (see Table I). It is also found in the Lorenz system for $R_{BS} = 278.56$, $\sigma_{BS} = 30$, and $b_{BS} = 1$ [38]. A route from the Lorenz attractor to the Burke and Shaw attractor in the Lorenz system can be obtained using a single parameter μ as

$$\begin{aligned} R &= R_L (1 - \mu) + R_{BS} \mu, \\ \sigma &= \sigma_L (1 - \mu) + \sigma_{BS} \mu, \\ b &= b_L (1 - \mu) + b_{BS} \mu. \end{aligned} \quad (32)$$

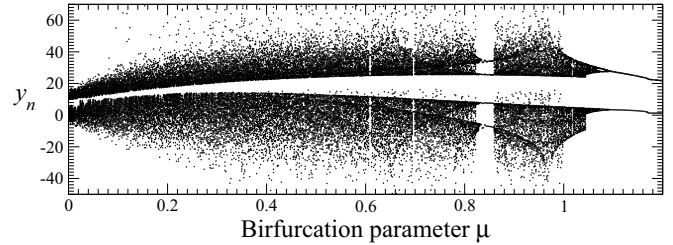


FIG. 7. Bifurcation diagram between the Lorenz attractor ($\mu = 0$) and the Burke and Shaw attractor ($\mu = 1$) in the Lorenz system.

The corresponding bifurcation diagram is plotted in Fig. 7(a). When $\mu > 1$, it is seen that the route to the Burke and Shaw attractor is as in the Burke and Shaw system, that is, there is a period-doubling cascade [36].

When μ is decreased, two simultaneous period-doubling cascades are observed, one being the symmetric of the other under the action of the rotation symmetry (a single one is plotted in Fig. 7). After an accumulation point for $\mu_\infty \approx 1.068$, the behavior becomes chaotic. Depending on the initial conditions, two coexisting symmetry-related attractors are observed. This feature persists up to an attractor merging crisis ($\mu_c \approx 1.045$) [36]. It corresponds to a boundary crisis between the two asymmetric attractors which merge into a symmetric one: there is therefore a sudden increase in the size of the attractor. This crisis appears when each attractor is characterized by a complete unimodal map, that is, when all periodic orbits predicted by the symbolic dynamics are actually realized within the attractor. Within this interval for the μ values, the bifurcation diagram can be fully predicted from the unimodal order [39,40].

The Burke and Shaw attractor [Fig. 8(a)], which is the symmetric attractor observed after the merging attractor crisis, is bounded by a genus-1 torus [Fig. 8(b)]. Consequently, the Poincaré section has a single component. We adjusted the R -parameter to have a first-return map made of four branches [Fig. 8(c)] and associated with a complete symbolic dynamics. It was shown that, when the symmetry is modded out, it corresponds to a complete unimodal map, [36] ensuring a certain kind of universality to this attractor. There are two joining lines in this attractor which can justify the use of a two-component Poincaré section [36]. Using the Poincaré section $\mathcal{P}_{z_{\max}}$ with the y variable, we obtained the first-return map plotted in Fig. 8(c): The important difference with the map computed for the Lorenz attractor is the lack of a branch crossing the first bisecting line, a signature of this symmetric genus-1 attractor. The two smooth unimodal maps are with a minimum due to an odd global torsion in each wing of the attractor. Indeed, the template for the Burke and Shaw [Fig. 8(d)] can be constructed from the template of a double-cover of the Rössler attractor with a global torsion of a π -twist in each wing. Note that the strip 1 and $\bar{1}$ are identical to those of the template for the Lorenz attractor. By merging these two template [Figs. 6(d) and 8(d)] lead to a six-strip template [Fig. 9] which describes most of the attractors produced by Lorenz-like system. It contains the Lorenz attractor, the Burke and Shaw attractor and all those which can be produced with six strips in the bifurcation diagram plotted in Fig. 7.

TABLE I. Governing equations and range of the rotation axis for which the transverse stability is of the saddle type; the structure of the jerk function induced by the variable x is also reported. Systems are ranked by increasing complexity.

	Ref.	n	Equations	n_{sp}	Range	Jerk function								
						X	Y	Z	X^3	X^2Y	X^2Z	XY^2	$\frac{Y^2}{X}$	$\frac{YZ}{X}$
Malasoma	[17]	5_2	$\begin{cases} \dot{x} = -ax + y \\ \dot{y} = xz \\ \dot{z} = 1 - x^2 \end{cases}$	2	$z > 0$	•	—	•	•	—	—	—	•	•
Malasoma	[17]	5_2	$\begin{cases} \dot{x} = y \\ \dot{y} = -ay + xz \\ \dot{z} = 1 - x^2 \end{cases}$	2	$a > 0$	•	—	•	•	—	—	—	•	•
Sprott B	[48]	5_2	$\begin{cases} \dot{x} = -x + ay \\ \dot{y} = xz \\ \dot{z} = 1 - xy \end{cases}$	2	$z > \frac{1}{a}$	•	—	•	•	•	—	—	•	•
Sprott C	[48]	5_2	$\begin{cases} \dot{x} = -x + ay \\ \dot{y} = xz \\ \dot{z} = 1 - y^2 \end{cases}$	2	$z > \frac{1}{a}$	•	—	•	•	•	—	•	•	•
Shimizu & Morioka	[49]	6_2	$\begin{cases} \dot{x} = y \\ \dot{y} = x - ay - xz \\ \dot{z} = -bz - x^2 \end{cases}$	3	$z < 1$	•	—	•	•	—	—	—	•	•
Liu & Yang	[50]	6_2	$\begin{cases} \dot{x} = -ax + ay \\ \dot{y} = bx - xz \\ \dot{z} = -cz + xy \end{cases}$	3	$z < \frac{a}{4} + b$	•	•	•	•	—	—	—	•	•
Kim & Chang	[47]	6_2	$\begin{cases} \dot{x} = -ax + ay \\ \dot{y} = by - xz \\ \dot{z} = -cz + x^2 \end{cases}$	3	$z < b$	•	•	•	•	—	—	—	•	•
Burke & Shaw	[37]	6_2	$\begin{cases} \dot{x} = -ax - ay \\ \dot{y} = -y - axz \\ \dot{z} = b + axy \end{cases}$	2	$z > \frac{1}{a}$	•	—	•	•	•	—	—	•	•
Lü & Chen	[51]	6_2	$\begin{cases} \dot{x} = -ax + ay \\ \dot{y} = by - xz \\ \dot{z} = -cz + xy \end{cases}$	3	$z < 0$	•	•	•	•	•	—	—	•	•
Lorenz	[1]	7_2	$\begin{cases} \dot{x} = -ax + ay \\ \dot{y} = bx - y - xz \\ \dot{z} = -cz + xy \end{cases}$	3	$z < R - 1$	•	•	•	•	•	—	—	•	•
Wang	[52]	7_2	$\begin{cases} \dot{x} = -ax + ay \\ \dot{y} = -y - xz \\ \dot{z} = b - z + xy \end{cases}$	3	$z < -1$	•	•	•	•	•	—	—	•	•
Vallis	[6,53,54]	7_2	$\begin{cases} \dot{x} = -ax + by \\ \dot{y} = -y + xz \\ \dot{z} = 1 - z - xy \end{cases}$	3	$z > \frac{a}{b}$	•	•	•	•	•	—	—	•	•
Chongxin <i>et al.</i>	[55]	7_3	$\begin{cases} \dot{x} = -ax + by \\ \dot{y} = bx - xz \\ \dot{z} = -cz + x^2 + dy^2 \end{cases}$	3	$z < b$	•	•	•	•	•	—	—	•	•
Rikitake	[4]	7_3	$\begin{cases} \dot{x} = -ax + yz \\ \dot{y} = -bx - ay + xz \\ \dot{z} = 1 - xy \end{cases}$	2	$z \in \mathbb{R} \setminus [\lambda_-; \lambda_+]$	•	•	•	•	•	•	•	•	•

$$\lambda_{\pm} = \frac{b \pm \sqrt{b^2 + 4a^2}}{2}$$

The template shown in Fig. 9 is described by the linker with

$$\mathcal{L}_{gL} = \begin{bmatrix} 0 & 0 & 0 & 0 & 0 & 0 \\ 0 & +1 & +1 & 0 & 0 & 0 \\ 0 & +1 & +2 & 0 & 0 & 0 \\ 0 & 0 & 0 & 0 & 0 & 0 \\ 0 & 0 & 0 & 0 & +1 & +1 \\ 0 & 0 & 0 & 0 & +1 & +2 \end{bmatrix}, \quad (33)$$

$$J_{ij} = \begin{bmatrix} 1 & \cdot & \cdot & \cdot & 3 & 2 \\ \cdot & 3 & 2 & 1 & \cdot & \cdot \end{bmatrix}. \quad (34)$$

Definition 2. A Lorenz-like attractor is globally invariant under a rotation symmetry and has at least four strips among the six of the template described by the linker \mathcal{L}_{gL} .

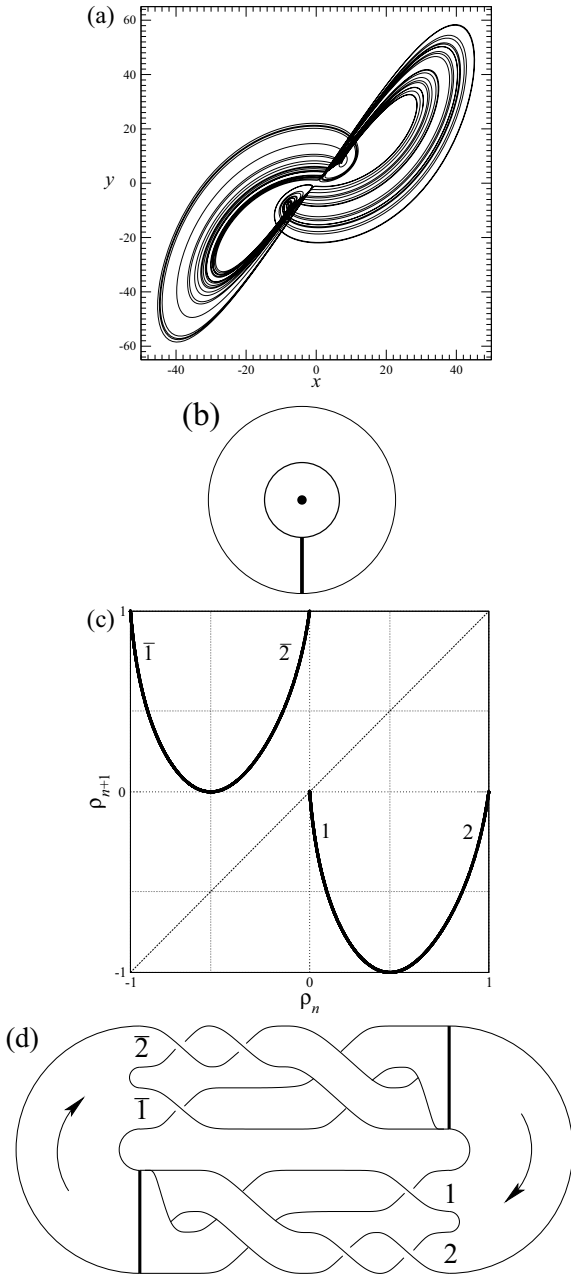


FIG. 8. (b) Genus-1 torus bounding the Burke and Shaw attractor (a) produced by the Lorenz system (4); (c) the first-return map to the one-component Poincaré section built from the normalized variable ρ_n (see the main text), and (d) the template describing its topology. The periodic orbits $(1\bar{0}\bar{1})$ and $(\bar{1}012)$ are drawn in the template. Parameter values: $R_{BS} = 278.56$, $\sigma_{BS} = 30$, and $b_{BS} = 1$.

C. The proto-Lorenz attractor

The Lorenz attractor can be viewed as the twofold cover of the proto-Lorenz attractor, that is, of an attractor without any residual symmetry. This was introduced by Miranda and Stone [41]. It can be easily obtained by using the coordinate transformation

$$\Upsilon_\kappa = \begin{cases} u = \text{Re}(x + iy)^\kappa, \\ v = \text{Im}(x + iy)^\kappa, \\ w = z, \end{cases} \quad (35)$$

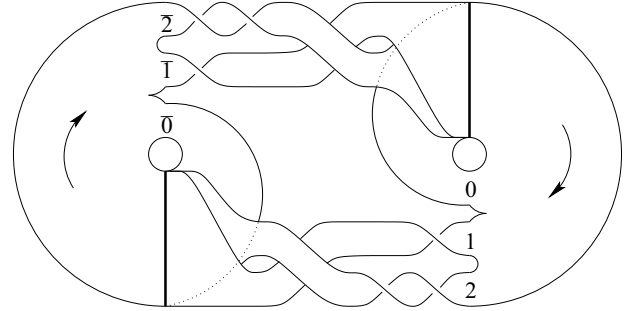


FIG. 9. Template for most of the Lorenz-like attractors produced by Lorenz-like systems.

where

$$\Upsilon_2 = \begin{cases} u = x^2 - y^2, \\ v = 2xy, \\ w = z, \end{cases} \quad (36)$$

when $\kappa = 2$, thus producing an attractor without any symmetry and bounded by a genus-1 torus [Fig. 10(a)]. It is called the image attractor of the Lorenz attractor. A first-return map to the Poincaré section

$$\mathcal{P}_{\text{proto}} = \{(u_n, v_n) \in \mathbb{R}^2 \mid w_n = R - 1, \dot{w}_n > 0\} \quad (37)$$

of the attractor produced by the proto-Lorenz system is the Lorenz map [Fig. 10(b)]: according to the terminology used in the taxonomy [24], this is a torn unimodal map. The topology of the proto-Lorenz attractor is described by a template with a single joining chart [Fig. 10(c)] and described by the linker

$$\mathcal{L}_{\text{pL}} = \begin{bmatrix} 0 & 0 \\ 0 & +1 \end{bmatrix}. \quad (38)$$

This template is in fact a subtemplate of the template for the Lorenz attractor [Fig. 6(d)].

The coordinate transformation Υ_κ is used to mod out an order- κ rotation symmetry $\mathcal{R}_z(\frac{2\pi}{\kappa})$. When it is inserted, v_κ^{-1} can be used to introduce such a symmetry, the z axis being the rotation axis. Consequently, every attractor being the κ -fold cover of the proto-Lorenz attractor is a Lorenz-like attractor. Some examples are treated elsewhere [41–43]. We will here limit ourselves to the case $\kappa = 2$. If the coordinate transformation (35) is applied to the Burke and Shaw attractor, then a smooth unimodal map is obtained (not shown). If it is applied to the attractor produced by the Lorenz system with the parameter values defined as in Eq. (32) and with $\mu = 0.5$, then a first-return map with more than two branches is obtained [Fig. 11(b)].

As introduced by Letellier and Gilmore [13], the location of the rotation axis with respect to the image attractor may induce inequivalent topologies. There are two typical cases: when the rotation axis is located at the critical point of the first-return map or in the nonvisited domain at the center of the attractor. The former leads to the Lorenz attractor and the latter will be discussed in Sec. IV D [13]. Only these two cases will be detailed here. Then, as suggested by Ghrist *et al.* [44], global torsion can be added to obtain Lorenz-like templates: this will be also briefly discussed.

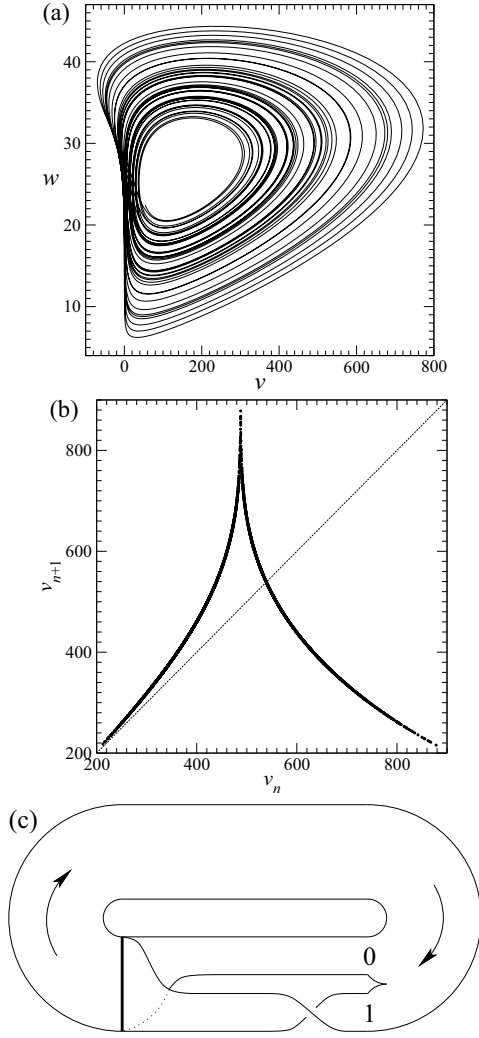


FIG. 10. Chaotic attractor (a) without any residual symmetry produced by the proto-Lorenz system with its torn unimodal map (b) and its template (c). Parameter values: $R = 28$, $\sigma = 10$, and $b = \frac{8}{3}$.

D. A genus-1 Lorenz attractor

To obtain the Lorenz attractor, the rotation axis crosses the attractor at a location which corresponds to the critical point of the map [13]. When the proto-Lorenz attractor is shifted, for instance, with the coordinate transformation $U \mapsto u - 85$, the rotation axis is in the nonvisited domain in the center of the proto-Lorenz attractor, and the two-fold cover is an attractor bounded by a genus-1 torus [Fig. 12(a)] [43]. This attractor has two joining charts resulting from the conjugation of two torn unimodal maps since, in a twofold cover, the dynamical units associated with the image is copied twice. A two-component Poincaré section is therefore justified and a four-branch first-return map is obtained [Fig. 12(c)]: This map has a structure resembling to the structure of the first-return map of the Burke and Shaw attractor [Fig. 8(d)], but the two unimodal maps are with a maximum (and not a minimum) since there is no odd global torsion in each wing. Moreover, each critical point is a cusp, a signature of the tearing and not a smooth extremum. Without any global torsion, the template

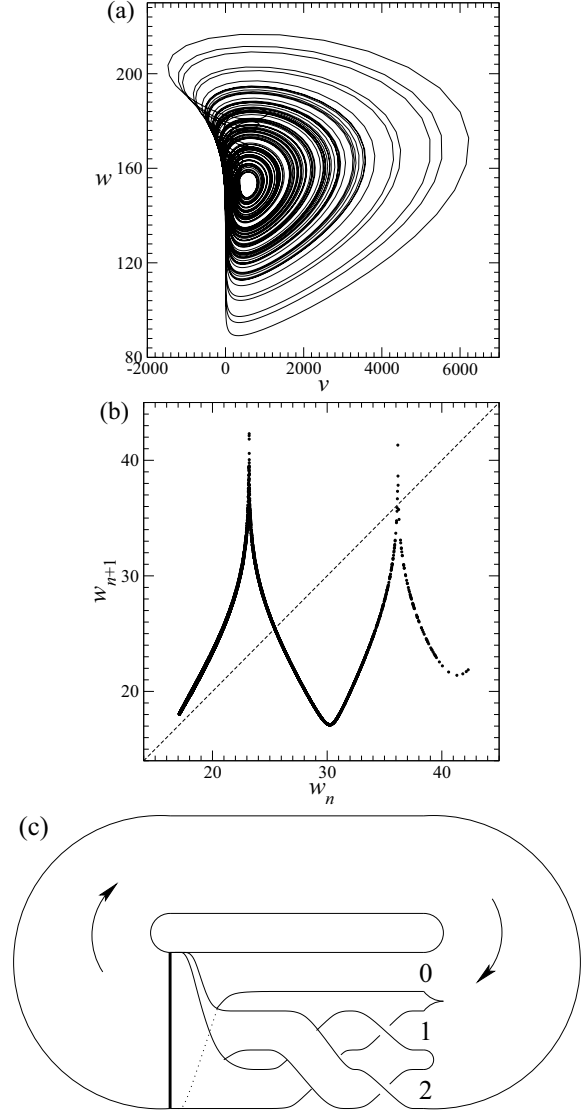


FIG. 11. Chaotic attractor (a) with its first-return map (b) produced by the proto-Lorenz system for $\mu = 0.5$. See Eq. (32) for the corresponding parameter values. The template (c) is drawn with the first three strips.

[Fig. 12(c)] is simpler than the template for the Burke and Shaw attractor [Fig. 8(d)], and can be described by the linker

$$\mathcal{L}_{Lg1} = \begin{bmatrix} 0 & 0 & 0 & 0 \\ 0 & +1 & 0 & 0 \\ 0 & 0 & +1 & +1 \\ 0 & 0 & +1 & +2 \end{bmatrix}, \tag{39}$$

with

$$J_{ij} = \begin{bmatrix} \cdot & \cdot & 1 & 2 \\ 1 & 2 & \cdot & \cdot \end{bmatrix}, \tag{40}$$

As it is derived from the proto-Lorenz attractor by introducing a rotation symmetry, this attractor can also be classified as a Lorenz-like attractor. Unfortunately, as far as our knowledge extends, this specific attractor has not been observed as being produced by a Lorenz-like system. There is an infinite number

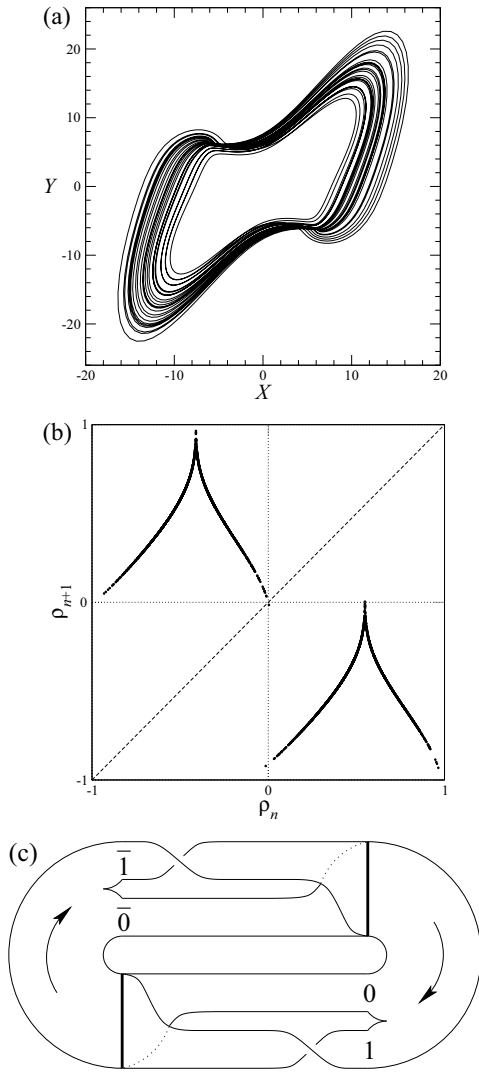


FIG. 12. A genus-1 Lorenz-like attractor (a) obtained from the twofold cover of the proto-Lorenz attractor whose rotation axis is close to the saddle-focus point around which the trajectory circles. (b) First-return map to a two-component Poincaré section. (c) Template. Parameter value as in Fig. 10.

of ways for constructing κ -fold cover of the proto-Lorenz attractor. The corresponding attractors are also Lorenz-like attractors; however, we encourage the reader to refer to the existing literature for further details [35,41,43].

E. The Moore-Spiegel attractor

There is an attractor which was first observed in a system proposed by Moore and Spiegel [45] and whose template was provided by Letellier [46]. The Moore-Spiegel system has an inversion symmetry and, consequently, it is not a Lorenz-like system. We therefore prefer to investigate this type of attractor in the Lorenz-like system in which we found it, that is, in the Kim and Chang system [47] (see Table I) whose complexity $n = 6_2$ is simpler than those of the Lorenz system.

The attractor—that we will designate as the Moore-Spiegel attractor—is potted in Fig. 13(a). It is bounded by a genus-3 torus as the Lorenz attractor (Fig. 6(b)) and, consequently, a

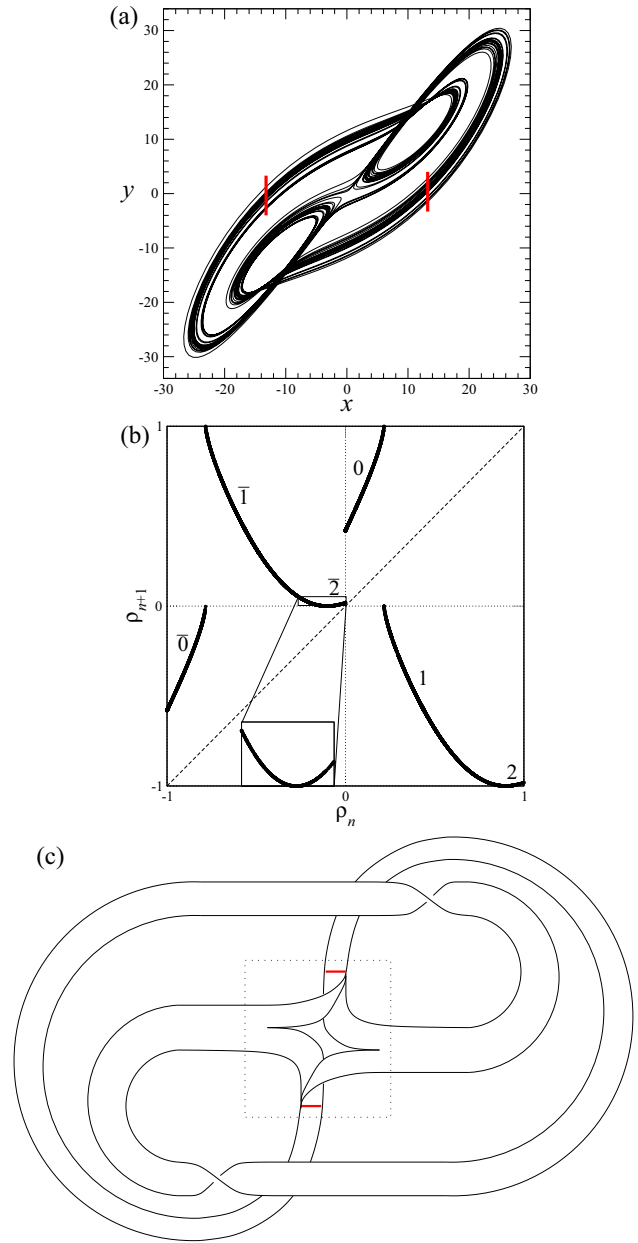


FIG. 13. The Moore-Spiegel attractor (a) produced by the Kim and Chang system. The two components of the Poincaré section are displayed as red thick lines, in each of the two wings of the attractor. The insert in panel (b) corresponding to the first-return map reveals a third branch in each wing whose corresponding strips are not drawn in the template (c). Parameter values: $a = 30$, $b = 15.89$, and $c = 11$.

two-component Poincaré section defined, for instance, as

$$\mathcal{P}_{KC} \equiv \{(y_n, z_n) \in \mathbb{R}^2 \mid x_n = \pm\sqrt{bc}, \dot{x}_n \leq 0, z_n > 26.5\} \tag{41}$$

is required. The z variable is thus normalized within the two unit intervals $] - 1, 0[$ and $] 0, 1[$. For the retained parameter values, there are six branches in the first-return map as those associated with the generalized template [Fig. 9]. A direct template is drawn in the x - y plane with only the four most developed strips labeled by $\bar{0}$, $\bar{1}$, 0 , and 1 [Fig. 13(c)]. There is one positive global torsion in each wing. In the central part

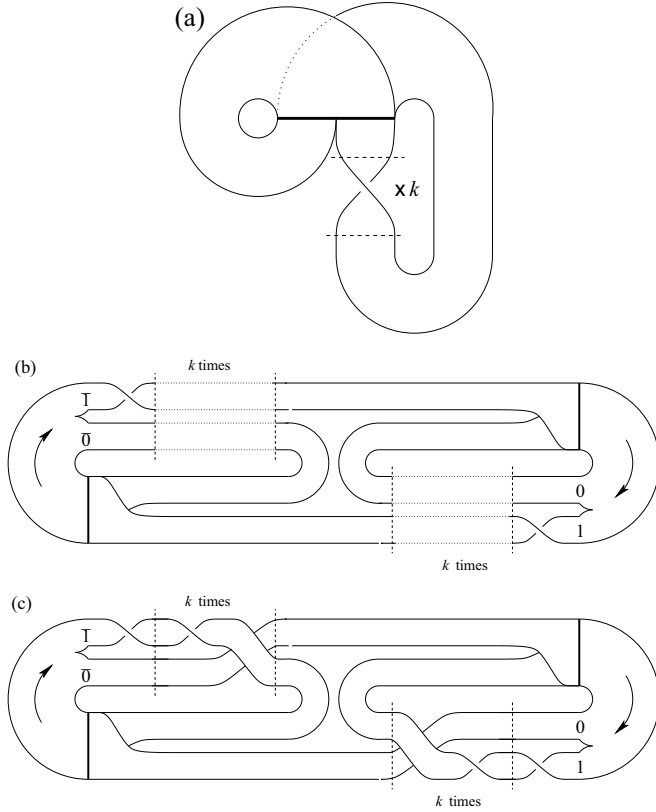


FIG. 14. Ghrist’s Lorenz-like template (a) and its symmetrized versions for k even (b) and k odd (c).

(within the dotted square), put the East and West strips along the rotation axis (perpendicular to the x - y plane) and leave the North and South strips in the x - y plane; then, rotate the central part by $-\pi$. Only the East and West strips gained a negative π -twist which can be moved toward the positive π -twist up to their cancellation through a Reidemeister move I. It then remains a template which is topologically equivalent to the template drawn for the Lorenz attractor [Fig. 6(d)]. The Moore-Spiegel attractor is therefore topologically equivalent to the Lorenz attractor. This equivalence leads us to the conclusion that the Moore-Spiegel attractor is obviously a Lorenz-like attractor.

F. Ghrist’s Lorenz-like template

In a study on universal template—a template which contains all the types of knots—Ghrist introduced the concept of Lorenz-like template as drawn in Fig. 14(a) [44]. Since we only considered symmetric attractors, we retained the symmetrized Lorenz-like template as drawn in Figs. 14(b) and 14(c). Note the dependence on the parity of the number k of π twists. The corresponding linker is thus

$$\mathcal{L}_{Lg1} = \begin{bmatrix} k & k & 0 & 0 \\ k & k+1 & 0 & 0 \\ 0 & 0 & k & k \\ 0 & 0 & k & k+1 \end{bmatrix}, \tag{42}$$

with

$$J_{ij} = \begin{bmatrix} 1 & \cdot & \cdot & 2 \\ \cdot & 2 & 1 & \cdot \end{bmatrix}, \tag{43}$$

for k even and with

$$J_{ij} = \begin{bmatrix} \cdot & 1 & \cdot & 2 \\ 2 & \cdot & 1 & \cdot \end{bmatrix}, \tag{44}$$

with k odd. In this work, the global torsion can be either positive or negative since we are not concerned with universal template. To the best of our knowledge, none of the known chaotic systems produces such an attractor with $k \neq 1$.

Through a simple generalization of the Ghrist Lorenz-like template to include six strips, the following linker is obtained:

$$\mathcal{L}_{L1} = \begin{bmatrix} k & k & k+1 & 0 & 0 & 0 \\ k & k+1 & k+1 & 0 & 0 & 0 \\ k & k+1 & k+2 & 0 & 0 & 0 \\ 0 & 0 & 0 & k & k & k+1 \\ 0 & 0 & 0 & k & k+1 & k+1 \\ 0 & 0 & 0 & k & k+1 & k+2 \end{bmatrix}, \tag{45}$$

with

$$J_{ij} = \begin{bmatrix} \cdot & 3 & 2 & 1 & \cdot & \cdot \\ 1 & \cdot & \cdot & \cdot & 3 & 2 \end{bmatrix}, \tag{46}$$

for k even and with

$$J_{ij} = \begin{bmatrix} \cdot & 2 & 1 & 3 & \cdot & \cdot \\ 3 & \cdot & \cdot & \cdot & 2 & 1 \end{bmatrix}, \tag{47}$$

with k odd. The Lorenz attractor corresponds to $k = 0$ without the strips $k + 2$ and $k + 2$, and the Burke and Shaw attractor to $k = 0$ without the strips k and k .

V. LORENZ-LIKE SYSTEMS

In this section, several well-known Lorenz-like systems are investigated. All of them fulfill the definition 1: the rotation axis is systematically associated with the z axis. The systems are reported in Table I. The jerk function induced by the variable x of each of them is written in the form

$$F_x = K_0 + K_1 X + K_2 Y + K_3 Z + K_4 X^2 + K_5 XY + K_6 XZ + K_7 Y^2 + K_8 YZ + K_9 Z^2 + K_{10} X^3 + K_{11} X^2 Y + K_{12} X^2 Z + K_{13} XY^2 + K_{23} \frac{Y^2}{X} + K_{24} \frac{YZ}{X}. \tag{48}$$

To the best of our knowledge, none of the known systems include the monomial $\alpha_{39} z^2$.

The Lorenz system, the Wang system, and the Vallis systems have jerk functions induced by the variable x which the same structure. Note that the Vallis system is equivalent to the system obtained for describing a water wheel [6,54]. The coefficients β_{ij} of the jerk function for the Wang system can be expressed as a function of the coefficients α_{ij} of the jerk

function of the Lorenz system as

$$\begin{aligned}
 \beta_{11} &= \alpha_{11}, \\
 \beta_{12} &= -\frac{\alpha_{12} \alpha_{21} \alpha_{33}}{\beta_{26} \beta_{30}}, \\
 \beta_{22} &= \alpha_{22}, \\
 \beta_{26} &= \alpha_{26}, \\
 \beta_{30} & \\
 \beta_{33} &= \alpha_{33}, \\
 \beta_{35} &= \frac{\alpha_{26} \alpha_{35}}{\beta_{26}},
 \end{aligned}
 \tag{49}$$

where β_{30} is a free parameter. There is therefore a diffeomorphism between the Lorenz and the Wang systems when $b = 1$; the Wang system is therefore a system whose parameter space is a restriction of the parameter space of the Lorenz system. Nevertheless, it can be shown that for any triplet of parameter values (R, σ, b) the Lorenz system can be rewritten as

$$\begin{aligned}
 \dot{x} &= -\frac{\sigma}{b}x + y, \\
 \dot{y} &= \frac{R\sigma}{b^2}x - \frac{1}{b}y - xz, \\
 \dot{z} &= -z + xy,
 \end{aligned}
 \tag{50}$$

that is, the Lorenz system can be reduced to a two-parameter system. This means also that the Wang system can produce every chaotic attractor produced by the Lorenz system.

The jerk equivalence was not found between the Vallis and the Lorenz systems, but it is possible to apply the coordinate transformation

$$\Phi = \begin{cases} x \mapsto x, \\ y \mapsto y, \\ z \mapsto z - \frac{\alpha_{21}}{\alpha_{26}}, \end{cases}
 \tag{51}$$

with α_i s being those of the Lorenz system (4) to the Lorenz system to obtain

$$\begin{aligned}
 \dot{x} &= \alpha_{11} x + \alpha_{12} y, \\
 \dot{y} &= \alpha_{22} y + \alpha_{26} xz, \\
 \dot{z} &= \frac{\alpha_{31}\alpha_{33}}{\alpha_{26}} + \alpha_{33} z + \alpha_{35} xy,
 \end{aligned}
 \tag{52}$$

which is thus rewritten in the form of the Vallis system. When the coefficients of the Lorenz system (4) are set to

$$\begin{aligned}
 \alpha_{11} &= -a & \alpha_{12} &= b, \\
 \alpha_{21} &= 1 & \alpha_{22} &= -1 & \alpha_{26} &= 1, \\
 \alpha_{33} &= -1 & \alpha_{35} &= -1,
 \end{aligned}
 \tag{53}$$

the Vallis system is derived. This establishes the diffeomorphic equivalence between the Lorenz and Vallis systems under Φ . As a result, the Lorenz, Wang, and Vallis systems are all considered to be diffeomorphically equivalent.

The two minimal systems proposed by Malasoma are diffeomorphically equivalent ($y \mapsto y - \frac{bx}{a}$) [17]. The Sprott B system is diffeomorphically equivalent to a system later proposed [58]. Among the six-monomials systems, the Lü and Chen system is the sole to produce a Lorenz attractor ($a = 36$, $b = 3$, and $c = 15$) but no diffeomorphism was found between

the Lorenz system and the Lü and Chen systems. Nevertheless, they can be combined with a single parameter—in a similar way as we did for the Lorenz attractor and the Burke and Shaw attractor with Eq. (32)—to switch from the Lorenz system to the Lü-Chen systems with a single parameter [59]. The Shimizu and Morioka system has the same algebraic structure as the Rucklidge system [60].

The Gissinger system (see Table II) has an algebraic complexity $n = 7_3$ (seven monomials with three nonlinear ones) and is equivalent to the system investigated by Lü, Chen, and Cheng [19], mostly for $c = 0$. With this null c coefficient, the symmetry is no longer a rotation symmetry but a \mathcal{V}_4 symmetry [61] and therefore the system is not a Lorenz-like system according to our definition. With $c = 0$, this system produces a Burke and Shaw attractor (see Fig. 9(b) in Ref. [61]). With $c \neq 0$, the \mathcal{V}_4 symmetry is broken and the system is equivariant under a rotation symmetry $\mathcal{R}_z(\pi)$ and is therefore a Lorenz-like system. This is further confirmed by the rotation axis that has a transverse stability of the saddle type for $z \in [-\frac{a+b}{2}; \frac{a+b}{2}]$, which, according to our definition, is a characteristic of a Lorenz-like system.

After a quick search, we found that the system produces a Burke and Shaw attractor (Fig. 15) but not its symmetric form. Indeed, the constant monomial c in the third equation breaks the possibility to find the companion attractor commonly observed in Lorenz-like systems, leading to the symmetric attractor shown in Fig. 15(a). Here, before the attractor merging crisis, the two symmetry-related attractor are not close of each other along a revolution but are located on either side of the singular point $x_0 = [0 \ 0 \ -\sqrt{ab}]^T$. Moreover, the merging attractor crisis occurs through a homoclinic bifurcation, leading to a very different attractor than the one observed in the Burke and Shaw system, or in the Lorenz system. Most of the attractors produced by the Gissinger system have the structure of the attractor plotted in Fig. 15(b), clearly more complex than the attractors commonly produced by Lorenz-like systems. The presence of the three nonlinearities combined with four other monomials unlocks the dynamics to these complex dynamics and the simple attractors are only observed for small domains of the parameter space. This system is therefore a Lorenz-like system which does not produce Lorenz-like attractor, *stricto sensu*, since they are only characterized by the sub-template drawn in Fig. 15(c).

Finally, it was shown that there are 17 different “ansatz” systems leading to the same jerk function induced by the variable x of the Lorenz system [10]. Among these 17 ansatz systems, some of them provide only the correct structure for the jerk function, but their coefficients cannot be expressed as a function of those from the Lorenz system; consequently, there is no proof for a diffeomorphism between these ansatz systems and the Lorenz system [16]. In this discussion, we will only consider the ansatz systems that exhibit diffeomorphic equivalence to the Lorenz system (4). This means that we will focus on systems where the relationships between the coefficients of the Lorenz system and the ansatz system can be expressed. Systems that are already known and equivalent to others will be excluded from the discussion. For instance, the ansatz system A_{11} reported in Table 1 of Ref. [10] is the Vallis system discussed above. It is thus possible to add seven

TABLE II. Lorenz-like systems with a broken \mathcal{V}_4 symmetry.

Lü, Chen & Cheng	[19]	6_3	$\begin{cases} \dot{x} = \frac{ab}{a+b}x - yz \\ \dot{y} = -ay + xz \\ \dot{z} = -bz + xy \end{cases}$	1	$z \in [-a\sqrt{\frac{b}{a+b}}; a\sqrt{\frac{b}{a+b}}]$
Gissinger	[56]	7_3	$\begin{cases} \dot{x} = ax - yz \\ \dot{y} = -by + xz \\ \dot{z} = c - z + xy \end{cases}$	5	$z \in [-\frac{a+b}{2}; \frac{a+b}{2}]$
Leipnik & Newton	[57]	8_3	$\begin{cases} \dot{x} = -ax + y + byz \\ \dot{y} = -x - ay + bxz \\ \dot{z} = cz - bxy \end{cases}$	5	$z \in \mathbb{R} \setminus [-\frac{\sqrt{a^2+1}}{a+b}; \frac{\sqrt{a^2+1}}{a+b}]$

Lorenz-like systems (Table III) which are diffeomorphically equivalent to the Lorenz system. All the systems with an algebraic complexity $n = 7_3$ only differ by their linear parts. Indeed, all of them have the three nonlinearities as follows: the monomial xy in the second equation and the monomials x^2 and xy in the third equation. The ansatz system A_{10} and A_{11} only differ from the constraints between the coefficients: strictly speaking, they should be considered as the same system. The ansatz A_{14} has the same algebraic structure as the Lorenz system but with different constraints on the coefficients: this is not exactly a new system. In summary, there are five additional Lorenz-like systems that can be included alongside those listed in Table I.

VI. A NON-LORENZ-LIKE SYSTEM

There is a cubic system which was introduced by Arnéodo, Coulet, and Tresser to describe a different route to a Lorenz attractor [62]. The system reads

$$\begin{aligned} \dot{x} &= ax - ay, \\ \dot{y} &= -4ay + xz + bx^3, \\ \dot{z} &= -acz + xy + dz^2. \end{aligned} \tag{54}$$

With eight monomials, it exceeds the maximum limit set by our definition of Lorenz-like systems. The jerk function of the

TABLE III. Governing equations of some ansatz systems which are diffeomorphically equivalent to the Lorenz system with the same jerk function F_x . The range of the rotation axis for which the transverse stability is of the saddle type is reported when the free parameters are set to 1.

	Equations	Range
A_7	$\begin{cases} \dot{x} = \alpha_{12} y \\ \dot{y} = -(\sigma + 1)y + \alpha_{26} xz \\ \dot{z} = \frac{b\sigma(R-1)}{\alpha_{12} \alpha_{26}} - bz - \frac{\sigma}{\alpha_{12} \alpha_{26}} x^2 - \frac{1}{\alpha_{26}} xy \end{cases}$	$z > -\frac{(\sigma+1)^2}{4}$
A_8	$\begin{cases} \dot{x} = \alpha_{12} y \\ \dot{y} = \frac{\sigma(R-1)}{\alpha_{12}} x - (\sigma + 1)y + \alpha_{26} xz \\ \dot{z} = -bz - \frac{\sigma}{\alpha_{12} \alpha_{26}} x^2 - \frac{1}{\alpha_{26}} xy \end{cases}$	$z > -\sigma R + \frac{3}{4} - \frac{(\sigma+1)^2}{4}$
A_9	$\begin{cases} \dot{x} = -(\sigma + 1)x + \alpha_{12} y \\ \dot{y} = \alpha_{26} xz \\ \dot{z} = \frac{b\sigma(R-1)}{\alpha_{12} \alpha_{26}} - bz + \frac{1}{\alpha_{12} \alpha_{26}} x^2 - \frac{1}{\alpha_{26}} xy \end{cases}$	$z > -\frac{(\sigma+1)^2}{4}$
A_{10}	$\begin{cases} \dot{x} = \lambda_{\pm} x - \frac{\lambda_{\pm}}{\alpha_{26}\alpha_{34}} y \\ \dot{y} = \lambda_{\pm} y + \alpha_{26} xz \\ \dot{z} = -bz + \alpha_{34} x^2 - \frac{1}{\alpha_{26}} xy \end{cases}$	
A_{11}	$\begin{cases} \dot{x} = -\sigma x + \frac{bR\sigma}{\alpha_{26}\alpha_{30}} y \\ \dot{y} = -y + \alpha_{26} xz \\ \dot{z} = -bz + \alpha_{34} x^2 - \frac{1}{\alpha_{26}} xy \end{cases}$	
A_{12}	$\begin{cases} \dot{x} = -(\sigma + 1)x + \alpha_{12} y \\ \dot{y} = \frac{\sigma(R-1)}{\alpha_{12}} x + \alpha_{26} xz \\ \dot{z} = -bz + \frac{1}{\alpha_{12}\alpha_{26}} x^2 - \frac{1}{\alpha_{26}} xy \end{cases}$	
A_{14}	$\begin{cases} \dot{x} = -\sigma x + \frac{\sigma R}{\alpha_{21}} y \\ \dot{y} = \alpha_{21} x - y - \frac{1}{\alpha_{35}} xz \\ \dot{z} = -bz + \alpha_{35} xy \end{cases}$	
	$\lambda_{\pm} = \frac{-(\sigma+1) \pm \sqrt{4\sigma\rho + (\sigma-1)^2}}{2}$	

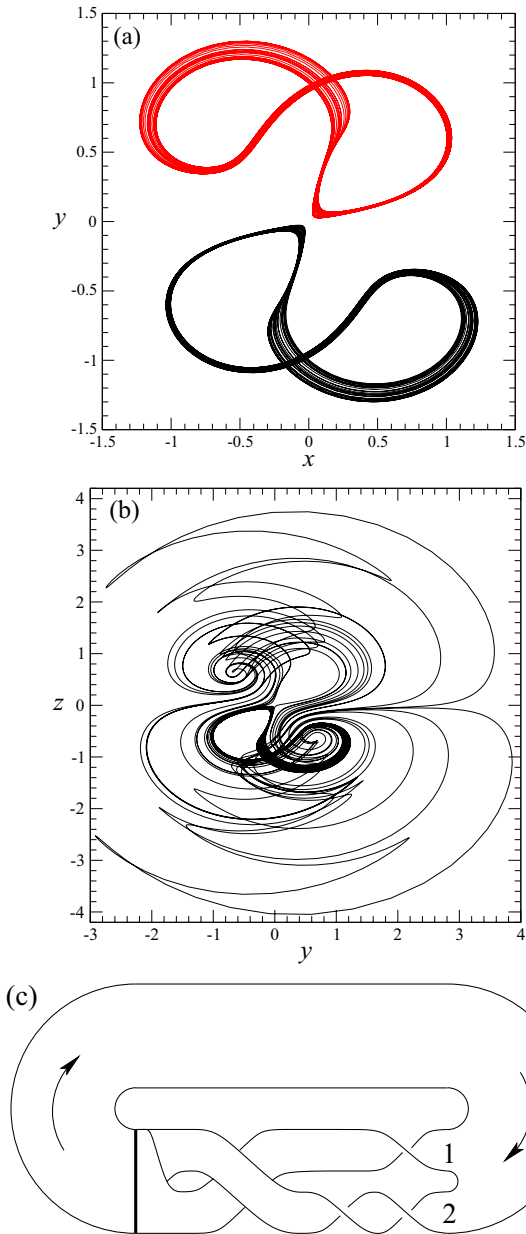


FIG. 15. Burke and Shaw attractor (a) before ($a = b = 0.2806$) and (b) after ($a = b = 0.2807$) the merging attractor crisis produced by the Gissinger system. The template (c) for the attractor before the merging attractor crisis is a sub-template of the template for the Burke and Shaw attractor [Fig. 8(d)]. Other parameter value: $c = 0.1$.

ACT system (54) is

$$F_x = \kappa_1 X + \kappa_2 Y + \kappa_3 Z + \kappa_4 X^3 + \kappa_5 X^2 Y + \kappa_6 X^2 Z + \kappa_7 X^5 + \kappa_8 \frac{Y^2}{X} + \kappa_9 \frac{YZ}{X} + \kappa_{10} \frac{Z^2}{X}, \quad (55)$$

which is a function more complex (higher degree, more numerous monomials) than the jerk function observed for the Lorenz-like systems. Such complexity enables the generation of three Lorenz-like attractors: the Lorenz attractor itself [Fig. 16(a)], the Burke and Shaw attractor [Fig. 16(b)], and the Moore-Spiegel attractor [Fig. 16(c)].

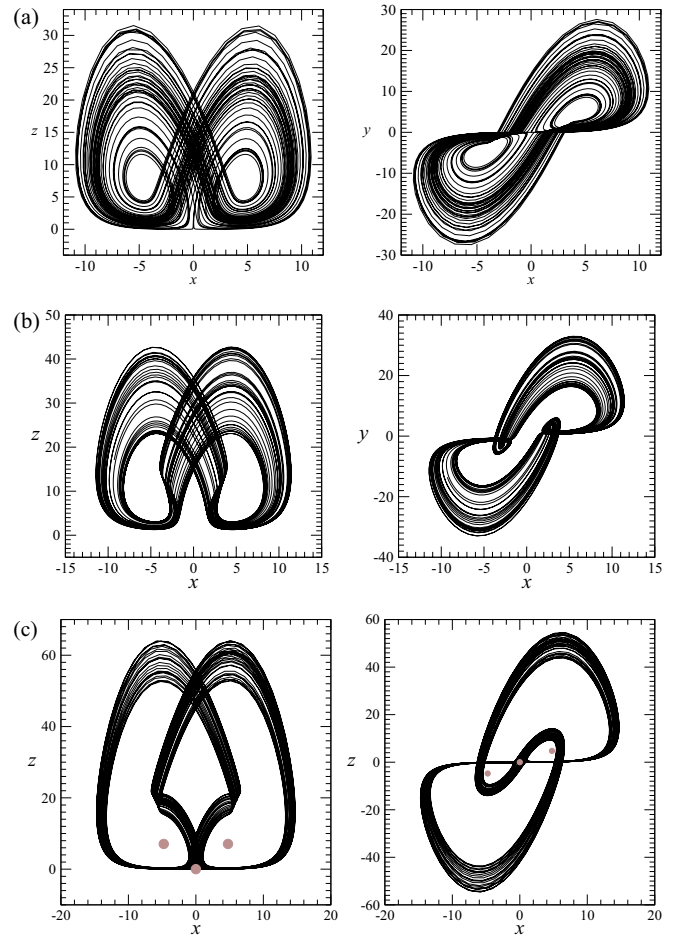


FIG. 16. Lorenz-like attractors produced by the ACT system. (a) Lorenz: $b = 0.000517$, and $c = 1.7$. (b) Burke and Shaw: $b = 0.0001$, and $c = 1.425$. (c) Moore and Spiegel: $b = 0.00517$, and $c = 1.7$. Other parameter values: $a = 1.8$ and $d = -0.02$.

VII. CONCLUSION

The exploration of systems exhibiting algebraic structures resembling the Lorenz system has been a prominent area of research since its emergence in the 1970s. These systems have presented intriguing outcomes, with some yielding attractors identical to the Lorenz system, while others showcasing distinct attractor dynamics. Surprisingly, certain systems that deviate significantly from the Lorenz system have produced attractors reminiscent of the iconic Lorenz attractor.

To provide a systematic approach to these phenomena, a definition was proposed for Lorenz-like systems. These systems are characterized by sets of ordinary differential equations that share a similar algebraic structure with the original Lorenz equations. Three specific properties were considered: (i) no more than seven monomials, (ii) quadratic nonlinearities, and (iii) a rotation symmetry of π . Thirteen chaotic systems from the literature and five additional systems resulting from an ansatz library were listed.

The systems discussed in this context all generate chaotic attractors that possess global invariance under the rotation symmetry and exhibit certain topological properties. These properties can often be synthesized using a six-strip tem-

plate. To designate these attractors, we propose the term “Lorenz-like attractors.” Among these attractors, there are three commonly represented types: the Lorenz attractor, the Burke and Shaw attractor, and the Moore-Spiegel attractor. Each of these reference attractors can be seen as a twofold cover of an attractor characterized by a unimodal map, which can have either a differentiable extremum or a cusp.

These three types of attractors serve as a basis, with other attractors often interpreted as combinations of two reference attractors. It is important to note that the first-return map of these attractors should be computed using a two-component Poincaré section due to the presence of two joining lines in the attractor. Furthermore, the computation should involve an equivariant variable, meaning a variable that is mapped

to its opposite under the rotation symmetry. To enhance the readability of the map, normalizing this variable onto two unit intervals is recommended.

We strongly encourage dynamicists to verify these properties before classifying an attractor as a Lorenz-like attractor.

The data used in this work were generated by basic code that integrates the systems under study using a Runge-Kutta integration scheme.

ACKNOWLEDGMENTS

E.M.A.M.M. acknowledges financial support from CNPq (Grants No. 310788/2021-8 and No. 405419/2021-0) and FAPEMIG (Grant No. APQ-03197-18).

-
- [1] E. N. Lorenz, Deterministic nonperiodic flow, *J. Atmos. Sci.* **20**, 130 (1963).
 - [2] J. B. McLaughlin and P. C. Martin, Transition to turbulence in a statically stressed fluid system, *Phys. Rev. A* **12**, 186 (1975).
 - [3] E. N. Lorenz, Predictability: Does the flap of a butterfly’s wings in Brazil set off a tornado in Texas? in *Proceedings of the 139th Meeting of the American Association for the Advancement of Science* (American Association for the Advancement of Science, Washington DC, 1972).
 - [4] T. Rikitake, Oscillations of a system of disk dynamos, *Math. Proc. Cambridge Philos. Soc.* **54**, 89 (1958).
 - [5] A. E. Cook and P. H. Roberts, *Math. Proc. Cambridge Philos. Soc.* **68**, 547 (1970).
 - [6] W. V. R. Malkus, Nonperiodic convection at high and low Prandtl number, *Mem. Soc. R. Sci. Liege* **4**, 125 (1972).
 - [7] H. Haken, Analogy between higher instabilities in fluids and lasers, *Phys. Lett. A* **53**, 77 (1975).
 - [8] L. Stenflo, Generalized Lorenz equations for acoustic-gravity waves in the atmosphere, *Phys. Scr.* **53**, 83 (1996).
 - [9] R. Festa, A. Mazzino, and D. Vincenzi, Lorenz-like systems and classical dynamical equations with memory forcing: An alternate point of view for singling out the origin of chaos, *Phys. Rev. E* **65**, 046205 (2002).
 - [10] C. Lainscsek, A class of Lorenz-like systems, *Chaos* **22**, 013126 (2012).
 - [11] X. Wang and G. Chen, A gallery of Lorenz-like and Chen-like attractors, *Int. J. Bifurcat. Chaos* **23**, 1330011 (2013).
 - [12] S. Wang, J. Kuang, J. Li, Y. Luo, H. Lu, and G. Hu, Chaos-based secure communications in a large community, *Phys. Rev. E* **66**, 065202(R) (2002).
 - [13] C. Letellier and R. Gilmore, Covering dynamical systems: Twofold covers, *Phys. Rev. E* **63**, 016206 (2000).
 - [14] T. D. Tsankov and R. Gilmore, Topological aspects of the structure of chaotic attractors in \mathbb{R}^3 , *Phys. Rev. E* **69**, 056206 (2004).
 - [15] C. Letellier and L. A. Aguirre, Investigating nonlinear dynamics from time series: The influence of symmetries and the choice of observables, *Chaos* **12**, 549 (2002).
 - [16] E. M. A. M. Mendes, C. Lainscsek, and C. Letellier, Diffeomorphical equivalence vs topological equivalence among Sprott systems, *Chaos* **31**, 083126 (2021).
 - [17] J.-M. Malasoma, New Lorenz-like chaotic flows with minimal algebraic structure, *Indian J. Industr. Appl. Math.* **1**, 1 (2008).
 - [18] C. Letellier, P. Dutertre, and G. Gouesbet, Characterization of the Lorenz system, taking into account the equivariance of the vector field, *Phys. Rev. E* **49**, 3492 (1994).
 - [19] J. Lü, G. Chen, and D. Cheng, A new chaotic system and beyond: The generalized Lorenz-like system, *Int. J. Bifurcat. Chaos* **14**, 1507 (2004).
 - [20] S. Yu, J. Lü, W. K. S. Tang, and G. Chen, A general multiscroll Lorenz system family and its realization via digital signal processors, *Chaos* **16**, 033126 (2006).
 - [21] C. Letellier and J.-M. Malasoma, Architecture of chaotic attractors for flows in the absence of any singular point, *Chaos* **26**, 063115 (2016).
 - [22] G. Byrne, R. Gilmore, and C. Letellier, Distinguishing between folding and tearing mechanisms in strange attractors, *Phys. Rev. E* **70**, 056214 (2004).
 - [23] O. E. RöSSLer, An equation for continuous chaos, *Phys. Lett. A* **57**, 397 (1976).
 - [24] C. Letellier, N. Stankevich, and O. E. RöSSLer, Dynamical taxonomy: Some taxonomic ranks to systematically classify every chaotic attractor, *Int. J. Bifurcat. Chaos* **32**, 2230004 (2022).
 - [25] T. D. Tsankov and R. Gilmore, Strange attractors are classified by bounding tori, *Phys. Rev. Lett.* **91**, 134104 (2003).
 - [26] M. Rosalie and C. Letellier, Systematic template extraction from chaotic attractors: I. Genus-one attractors with an inversion symmetry, *J. Phys. A* **46**, 375101 (2013).
 - [27] O. E. RöSSLer, Chaotic behavior in simple reaction system, *Z. Naturforsch. A* **31**, 259 (1976).
 - [28] J. Birman and R. F. Williams, Knotted periodic orbits in dynamical systems I. Lorenz’s equations, *Topology* **22**, 47 (1983).
 - [29] G. B. Mindlin, X.-J. Hou, H. G. Solari, R. Gilmore, and N. B. Tufillaro, Classification of strange attractors by integers, *Phys. Rev. Lett.* **64**, 2350 (1990).
 - [30] G. B. Mindlin, H. G. Solari, M. A. Natiello, R. Gilmore, and X.-J. Hou, Topological analysis of chaotic time series data from the Belousov-Zhabotinskii reaction, *J. Nonlinear Sci.* **1**, 147 (1991).
 - [31] G. B. Mindlin and R. Gilmore, Topological analysis and synthesis of chaotic time series, *Physica D* **58**, 229 (1992).

- [32] N. B. Tufillaro, T. Abbott, and J. Reilly, *An Experimental Approach to Nonlinear Dynamics and Chaos* (Addison-Wesley, Redwood City, CA, 1992).
- [33] G. D. Charó, C. Letellier, and D. Sciamarella, Temples: A bridge between homologies and templates for chaotic attractors, *Chaos* **32**, 083108 (2022).
- [34] L. Le Sceller, C. Letellier, and G. Gouesbet, Algebraic evaluation of linking numbers of unstable periodic orbits in chaotic attractors, *Phys. Rev. E* **49**, 4693 (1994).
- [35] C. Letellier, P. Dutertre, and B. Maheu, Unstable periodic orbits and templates of the Rössler system: Toward a systematic topological characterization, *Chaos* **5**, 271 (1995).
- [36] C. Letellier, P. Dutertre, J. Reizner, and G. Gouesbet, Evolution of multimodal map induced by an equivariant vector field, *J. Phys. A* **29**, 5359 (1996).
- [37] R. Shaw, Strange attractor, chaotic behavior and information flow, *Z. Naturforsch A* **36**, 80 (1981).
- [38] C. Letellier, T. D. Tsankov, G. Byrne, and R. Gilmore, Large-scale structural reorganization of strange attractors, *Phys. Rev. E* **72**, 026212 (2005).
- [39] P. Collet and J.-P. Eckmann, in *Iterated Maps on the Interval as Dynamical Systems*, Progress in Physics, edited by A. Jaffe and D. Ruelle (Birkhäuser, Boston/Berlin, 1981), Vol. 1.
- [40] C. Letellier and J.-M. Malasoma, Unimodal order in the image of the simplest equivariant jerk system, *Phys. Rev. E* **64**, 067202 (2001).
- [41] R. Miranda and E. Stone, The proto-Lorenz system, *Phys. Lett. A* **178**, 105 (1993).
- [42] C. Letellier and G. Gouesbet, Topological characterization of a system with high-order symmetries: the proto-Lorenz system, *Phys. Rev. E* **52**, 4754 (1995).
- [43] R. Gilmore and C. Letellier, *The Symmetry of Chaos* (Oxford University Press, New York, NY, 2007).
- [44] R. W. Ghrist, Branched two-manifolds supporting all links, *Topology* **36**, 423 (1997).
- [45] D. W. Moore and E. A. Spiegel, A thermally excited non-linear oscillator, *Astrophys. J.* **143**, 871 (1966).
- [46] C. Letellier, Caractérisation topologique et reconstruction des attracteurs étranges, Ph.D. thesis, University of Paris VII, Paris, France, 1994.
- [47] D. Kim and P. Hun Chang, A new butterfly-shaped chaotic attractor, *Results Phys.* **3**, 14 (2013).
- [48] J. C. Sprott, Some simple chaotic flows, *Phys. Rev. E* **50**, R647, (1994).
- [49] T. Shimizu and N. Morioka, On the bifurcation of a symmetric limit cycle to an asymmetric one in a simple model, *Phys. Lett. A* **76**, 201 (1980).
- [50] Y. Liu and Q. Yang, Dynamics of a new Lorenz-like chaotic system, *Nonlin. Anal.: Real World Appl.* **11**, 2563 (2010).
- [51] J. Lü and G. Chen, A new chaotic attractor coined, *Int. J. Bifurcat. Chaos* **12**, 659 (2002).
- [52] Y. Wang, Jonathan Singer, and Haim H. Bau, Controlling chaos in a thermal convection loop, *J. Fluid Mech.* **237**, 479 (1992).
- [53] G. K. Vallis, Conceptual models of El Niño and the southern oscillation, *J. Geophys. Res. [Oceans]* **93**, 13979 (1988).
- [54] L. E. Matson, The Malkus-Lorenz water wheel revisited, *Am. J. Phys.* **75**, 1114 (2007).
- [55] L. Chongxin, L. Ling, L. Tao, and L. Peng, A new butterfly-shaped attractor of Lorenz-like system, *Chaos Solitons Fractals* **28**, 1196 (2006).
- [56] C. Gissinger, A new deterministic model for chaotic reversals, *Eur. Phys. J. B* **85**, 137 (2012).
- [57] R. B. Leipnik and T. A. Newton, Double strange attractors in rigid body motion with linear feedback control, *Phys. Lett. A* **86**, 63 (1981).
- [58] G. van der Schrier and L. R. M. Maas, The diffusionless Lorenz equations: Shil'nikov bifurcations and reduction to an explicit map, *Physica D* **141**, 19 (2000).
- [59] J. Lu, G. Chen, D. Cheng, and S. Celikovský, Bridge the gap between the Lorenz system and the Chen system, *Int. J. Bifurcat. Chaos* **12**, 2917 (2002).
- [60] A. M. Rucklidge, Chaos in models of double convection, *J. Fluid Mech.* **237**, 209 (1992).
- [61] C. Letellier and R. Gilmore, Symmetry groups for 3D dynamical systems, *J. Phys. A* **40**, 5597 (2007).
- [62] A. Arnéodo, P. Couillet, and C. Tresser, A possible new mechanism for the onset of turbulence, *Phys. Lett. A* **81**, 197 (1981).